THE
PHYSICAL REVIEW

A journal of experimental and theoretical physics established by E. L. Nichols in 1893

SECOND SERIES, VOL. 181, NO. 2 10 MAY 1969

Determination of Exchange Interactions between Coupled Co^{2+} Ions in MgF_2 by Far-Infrared Spectroscopy

E. BELORIZKY,* S. C. NG,† AND T. G. PHILLIPS‡
Clarendon Laboratory, Oxford University, Oxford, England
(Received 22 October 1968)

We report here a far-infrared spectroscopy experiment in which we observe absorption lines due to pairs and triads of magnetic ions. A crystal of MgF_2 containing Co^{2+} ions substituted for Mg^{2+} is investigated and is found to show spectra due to next-nearest-neighbor Co^{2+} pairs, and also spectra due to groups of three Co^{2+} ions containing two next-nearest-neighbor bonds. The isotropic component of the pair exchange interaction is determined to be 9.8 cm^{-1}, and the anisotropic components are also evaluated. Identification and evaluation are carried out with the information obtained from the Zeeman effect. The exchange and Zeeman Hamiltonian matrices for pairs and triads are developed using symmetry considerations, and it is shown that magnetic dipole transitions are allowed and are of the correct strength to account for the observed spectra. It is also shown that the next-nearest-neighbor exchange constant found from the spin-wave dispersion curve for CoF_2 is in close agreement with the spectroscopic value found here.

I. INTRODUCTION

FAR-INFRARED spectroscopy provides a direct and powerful method for the study of exchange interactions between magnetic ions when they are incorporated as impurities of several percent concentration in diamagnetic host crystals. There is then a sensible probability that a magnetic ion will find a similar ion among its near neighbors or indeed that three or more magnetic ions may be clustered together. It is the purpose of this paper to describe the application of far-infrared spectroscopic techniques to one such system, i.e., Co^{2+} ions in MgF_2, and it is believed that this represents the first definite observation of far-infrared pair and triad spectra in a dilute magnetic system. Arguments are also presented to indicate possible reasons for the lack of previous observations of this type.

There are, of course, other techniques which have been used to obtain information about pair and triad spectra. Electron paramagnetic resonance[1,2] may be used to study the transitions within a given manifold, although it is difficult to obtain information concerning the isotropic component of the exchange energy. Such information can be obtained, however, by use of intensity measurements. Another useful method is optical spectroscopy. The most famous case is probably that of Cr^{3+} ions in Al_2O_3.[3] Here it is possible to observe $\Delta S=0$ electric dipole transitions between the exchange-coupled levels of pairs of magnetic ions in their ground states and the exchange levels arising from the same two ions when one is in the ground state and the other in an optically excited state. In practice, it turns out that these spectra are often hard to analyze. It might also be remarked that acoustic paramagnetic resonance[4] provides a further tool for investigation of weakly coupled ions.

We now briefly consider some of the essential features of far-infrared pair spectroscopy. This most direct method can only be used when the spectrum is either well above or well below the crystal reststrahl. As will be seen below, a light path through the crystal of the order of 10 cm is required even in the favorable materials, and in this case the wings of the electric dipole optical phonon absorption modes are most extensive. Also, great care must be taken to avoid confusion with the resonant phonon modes due to impurities, and it is essential to examine the magnetic field dependence of all modes suspected of being part of a coupled magnetic

* Permanent address: Laboratoire de Spectrométrie Physique associé au CNRS–Faculté des Sciences de Grenoble, France.
† Postdoctoral Fellow, National Research Council of Canada.
‡ Present address: Bell Telephone Laboratories, Murray Hill, N. J.
[1] J. H. E. Griffiths, J. Owen, J. G. Park, and M. F. Partridge, Proc. Roy. Soc. (London) **A250**, 84 (1959).
[2] M. T. Hutchings, R. J. Birgenau, and W. P. Wolf, Phys. Rev. **168**, 1026 (1968).
[3] A. L. Schawlow, D. L. Wood, and A. M. Clogston, Phys. Rev. Letters **3**, 271 (1959).
[4] R. Guermeur, J. Joffrin, A. Levelut, and J. Penné, Solid State Commun. **5**, 563 (1967); D. K. Garrod, H. M. Rosenberg, and J. K. Wigmore (to be published).

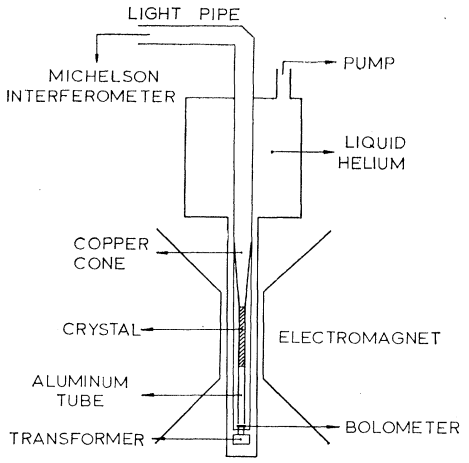

FIG. 1. Schematic diagram of the apparatus.

ion system.[5,6] A further most stringent requirement is that of a sizable transition probability. The somewhat limited signal-to-noise ratio available in the far infrared means that a transition probability comparable to normal magnetic dipole strength is required. We may consider under what general conditions this is possible.

If the exchange interaction between two neighboring ions is isotropic, then both electric and magnetic dipole transitions are essentially forbidden between levels whose spin differs by $\Delta S=\pm 1$. This might be expected to be approximately the case for ions with half-filled shells in their state of maximum multiplicity, e.g., Mn^{2+}, or for ions with a fully quenched orbital angular momentum leading to a singlet orbital ground state, such as the $^4A_2$ level of Cr^{3+} in Al_2O_3. It is well known, however, that when the orbital ground state of each ion is degenerate, the exchange interaction can be anisotropic.[7,8] Let us consider a case in which, after application of crystal-field and spin-orbit coupling, the ground state of each ion is a Kramers doublet described by effective spin $S=\frac{1}{2}$. An isotropic antiferromagnetic exchange coupling between two ions leads to an antisymmetric $S=0$ ground state and a symmetric $S=1$ excited state. If we suppose that the two ions have similar local symmetry and also high symmetry considered as a pair, then the anisotropic exchange is symmetric and, considered as a perturbation, may split the excited state into three singlets, each of which is still symmetric with respect to interchange of the two ions. Magnetic dipole transitions between the ground and excited states are still forbidden. However, if we lower the symmetry of the pair (e.g., by taking distant neighbors) such that antisymmetric anisotropic exchange coupling exists, then magnetic dipole transitions appear in first order, but since it is likely that the antisymmetric component of the exchange coupling will be only the order of, say, 10^{-1} of the isotropic component, we still have a negligible transition probability (i.e., 10^{-2} of magnetic dipole strength). Finally, let us make the local symmetry of the two ions magnetically inequivalent. If the "g" tensor of the single-ion Kramers doublet is anisotropic, which will be the case for local symmetry less than cubic and for unquenched orbital motion, then we have a definite zeroth-order magnetic dipole transition probability. These requirements led us to a study of coupled Co^{2+} ions in MgF_2, which, as will be seen in Sec. III, is a favorable case.

It should be mentioned that we have considered the possibility of electric dipole transitions between exchange-coupled ions using a similar mechanism to that proposed for far-infrared two-magnon absorption in antiferromagnetic fluorides.[9] This mechanism involves the spin-dependent effective dipole moment of the pair arising from the excitation of one ion to a state of odd parity and also the nondiagonal interionic exchange energy. When the interionic exchange coupling is anisotropic, the effective electric dipole moment is also anisotropic and has matrix elements between the pair states. However, an approximate calculation indicates that the electric dipole transition probability will always be at least one order of magnitude weaker than the magnetic dipole under the same conditions, given, of course, the usual energy separation, 10^4–10^5 cm^{-1}, to the first odd-parity state in ions of the iron-group series.

II. EXPERIMENTAL DETAILS

The very-far-infrared region of the electromagnetic spectrum (5–100 cm^{-1}) is usually regarded as the most difficult experimentally, particularly from the point of view of solid-state experiments. Although considerable technical advances have been made in recent years with regard to spectroscopic techniques[10,11] and to detector efficiency,[12–14] it is still true to say that the very low power available from spectral sources ($\sim 10^{-11}$ W/cm^{-1} bandwidth) severely limits the type of experiment which can be attempted at low energies. In order to make efficient use of available source power a spectrometer of the Michelson interferometric type was employed, and for an analysis of the advantages and disadvantages the reader is referred to the articles by Richards,[10] by Gebbie and Twiss,[11] and by Wheeler and Hill.[12]

[5] A system of spectral lines has been recently attributed to Ir^{4+} ions in the ammonium hexachloroplatinates, but the magnetic origin has not been established using the Zeeman effect: C. M. R. Platt and D. M. Martin, Chem. Phys. Letters **1**, 659 (1968).

[6] There is a preliminary report of the observation of the Zeeman effect of pair spectra of Co^{2+} ions in MgF_2: E. Belorizky, S. C. Ng, and T. G. Phillips, Phys. Letters **27A**, 489 (1968).

[7] P. M. Levy, Phys. Rev. **135**, A155 (1964).

[8] R. J. Elliott and M. F. Thorpe, J. Appl. Phys. **39**, 802 (1968).

[9] Y. Tanabe, T. Moriya, and S. Sugano, Phys. Rev. Letters **15**, 1023 (1965).

[10] P. L. Richards, J. Opt. Soc. Am. **54**, 1474 (1964).

[11] H. A. Gebbie and R. Q. Twiss, Rept. Progr. Phys. **29**, 729 (1966).

[12] R. G. Wheeler and J. C. Hill, J. Opt. Soc. Am. **56**, 657 (1966).

[13] A. J. Sievers and H. Marsh, Bull. Am. Phys. Soc. **13**, 668 (1968).

[14] M. A. Kinch and B. V. Rollin, Brit. J. Appl. Phys. **14**, 672 (1963).

A schematic diagram of the apparatus is shown in Fig. 1. Light from the low-pressure mercury vapor lamp was chopped mechanically at a frequency of 1 kc/sec and passed through the Michelson interferometer. The approximately plane-wave output was passed through a $\frac{3}{4}$-in.-i.d. light pipe and, by means of 45° reflecting mirrors, into the helium cryostat operating at 1.5°K. The light was then passed through a copper cone to the end of the MgF_2 crystal to be investigated. This crystal contained 5% Co^{2+} and was about 7 cm in length and grown on the [110] axis. The cross section was square and the whole was surrounded by a close-fitting aluminium tube which led down to the detector. A transverse magnetic field, at the site of the crystal, was available from a 15-in. Magnion electromagnet. This field was variable up to 28 kOe and could be rotated in the plane normal to the length of the crystal.

Although the crystal was only 7 cm in length, the approximate light path through it was 10 cm, since the light from the bottom of the cone was divergent. A geometric system designed to provide a fixed-angle cone of divergent light was tried, and gave almost identical results in terms of signal-to-noise ratio and absorption coefficient.

The light detector was of the Kinch-Rollin[14] type, consisting of a hot electron InSb bolometer with tuned transformer output to a low-noise valve amplifier. The bolometer and transformer were placed at the bottom of the cryostat, where they were screened from the dc magnetic field. For spectral energies of 3–30 cm^{-1}, the InSb bolometer was used, but for energies above 30 cm^{-1}, a doped Ge bolometer was found to be more efficient. In both cases the bolometer temperature was maintained at about 1.5°K.

III. SPECTROSCOPIC PROPERTIES OF Co^{2+} IONS IN MgF_2

MgF_2 is of the rutile-type crystal structure which is shown in Fig. 2. The Mg^{2+} ions form two interpenetrating tetragonal sublattices, each characterized by an environment rotated by 90° about the c (z) axis with respect to the other. Co^{2+} ions enter substitutionally for Mg^{2+} ions. We first consider in this section some well-known aspects of the single-ion spectrum, and go on to analyze the spectroscopic properties of exchange-coupled pairs of Co^{2+} ions and, finally, groups of three magnetic ions (triads).

A. Single Ion

The local environment of each Co^{2+} ion is basically a tetragonally distorted octahedron of fluorine ions, but with further rhombic distortions giving a point symmetry of D_{2h}. The $(3d)^7$ ground configuration of Co^{2+} gives rise to a ^4F free-ion ground state, which is then split by the cubic field into two orbital triplets and one singlet, and of these the $^4\Gamma_4$ triplet lies lowest. This $^4\Gamma_4$ state in fact contains a small admixture of the excited

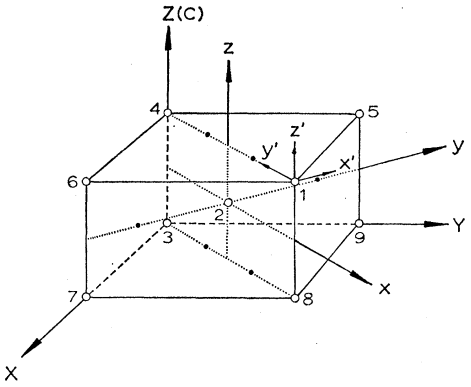

FIG. 2. Rutile structure. The open circles represent the Mg ions and the closed circles the fluorine ions. Axes x, y, and z refer to ion 2 and x', y', and z' to ion 1.

^4P state. Now the tetragonal distortion splits the $^4\Gamma_4$ state into a ^4E doublet and a $^4A_2$ singlet, and finally the effect of the rhombic distortion and spin-orbit coupling is to give six Kramers doublets, each belonging to the representation E of the D_{2h} double group. A level scheme is given in Fig. 3, where the energies of these six low-lying doublets are obtained from fluorescence spectra.[15]

EPR spectra[16] indicate that the principal values of the spectroscopic splitting factor g for the ground doublet are along the D_2 axes and have values $g_2^{xx}=g_1^{x'x'}=2.297$, $g_2^{yy}=g_1^{y'y'}=6.033$, and $g_2^{zz}=g_1^{z'z'}=4.239$ (the D_2 axes are $O_{x,y,z}$ and $O_{x',y',z'}$ for the two sites, respectively; see Fig. 2).

B. Exchange-Coupled Pairs

Our interest here centers on the next-nearest-neighbor (nnn) pairs of ions such as those of sites 1 and 2 in Fig. 2. We know from the case of the ordered antiferromagnet CoF_2, which has the same symmetry as MgF_2, that the nnn pair exchange energy is dominant over all

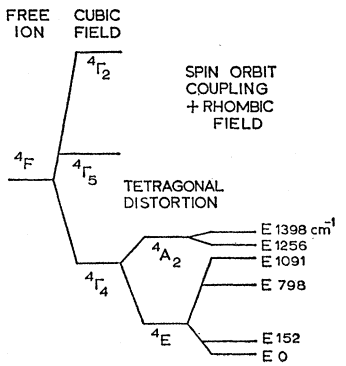

FIG. 3. Energy-level scheme showing the successive crystal field splitting of the ^4F free-ion ground state, due to (a) cubic field, (b) tetragonal distortion, and (c) spin-orbit coupling and rhombic field.

[15] L. F. Johnson, R. E. Deitz, and H. J. Guggenheim, Appl. Phys. Letters **5**, 21 (1964).
[16] H. M. Gladney, Phys. Rev. **143**, 198 (1966); **146**, 253 (1966).

other types of pairs.[17] Also, from the qualitative argument of the Introduction we may expect that this is the right type of pair to give a large transition probability for electromagnetic radiation.

We may examine the relative probability of finding such a pair in a normal distribution of substituted Co^{2+} ions in MgF_2. If we have a concentration c of Co^{2+} ions per Mg^{2+} ion, and if we consider an ion to be isolated if it has no magnetic ion as nn or nnn, then the probability of finding an isolated ion on any given site is $c(1-c)^{10}$, so we may expect $2c(1-c)^{10}$ isolated Co^{2+} ions per unit cell. Similarly, it is found that there are $c^2(1-c)^{14}$ and $8c^2(1-c)^{16}$ nn (type 1-8, Fig. 2) and nnn (type 1-2) ion pairs, respectively, per unit cell. For a Co^{2+} concentration of 5%, the ratio of nnn pairs to the number of isolated ions is about 15%.

In the experiment it is necessary to examine the magnetic field dependence of all lines found in the spectrum in order to establish beyond doubt their connection with a pair system. We therefore need to write down the form of the spin-dependent interactions between the ions of a pair and also an expression for the Zeeman effect.

1. Spin-Dependent Interactions

The spin-dependent interactions are dominated by exchange effects, although, of course, magnetic dipole coupling is present. In this paper the "exchange Hamiltonian" should be taken as a general Hamiltonian for all spin-spin interactions. The real exchange parameters will have to be extracted by making corrections for the small dipolar effects which can easily be calculated.

The form of the exchange interaction is governed by the symmetry. For a pair of nnn ions, the simple symmetry group contains only two elements, E and σ_v, i.e., the identity operator and a reflection in a vertical plane containing the pair (plane zox of Fig. 2). This group C_{1h} or C_s has only two one-dimensional representations Γ_1 and Γ_2, which are symmetric and antisymmetric, respectively, with respect to σ_v. The exchange interaction between the two Co^{2+} ions in their ground states must be invariant under σ_v. Introducing a pseudospin $S=\frac{1}{2}$ for each Kramers doublet, we see that S_{1y} and S_{2y} transform like Γ_1, and S_{1x}, S_{2x}, S_{1z}, and S_{2z} transform like Γ_2, so that the most general bilinear spin-dependent interaction is of the form

$$\mathcal{H}_{ex}=\mathbf{S}_1\cdot\mathbf{J}\cdot\mathbf{S}_2, \tag{1}$$

where the nonzero independent elements of J are J_{xx}, J_{yy}, J_{zz}, J_{zx}, and J_{xz}, and the pair axes are taken as for ion 2.

With total spin $\mathbf{S}=\mathbf{S}_1+\mathbf{S}_2$ we write the matrix elements of $\mathcal{H}_{ex}$ in the basis $|S,M_s\rangle$ and define some anisotropy elements which will be used throughout the rest of the paper. The Hamiltonian matrix becomes

$$\mathcal{H}_{ex}=\begin{array}{c} \\ \langle 1,1| \\ \langle 1,0| \\ \langle 1,-1| \\ \langle 0,0| \end{array}\begin{array}{c} \begin{array}{cccc} |1,1\rangle & |1,0\rangle & |1,-1\rangle & |0,0\rangle \end{array} \\ \begin{pmatrix} D+\frac{1}{4}J & \alpha & E & \beta \\ \alpha & -2D+\frac{1}{4}J & -\alpha & 0 \\ E & -\alpha & D+\frac{1}{4}J & \beta \\ \beta & 0 & \beta & -\frac{3}{4}J \end{pmatrix} \end{array}, \tag{2}$$

where J is the isotropic component (assumed to be antiferromagnetic) defined by

$$J=\tfrac{1}{3}(J_{xx}+J_{yy}+J_{zz}), \quad J>0 \tag{3}$$

and

$$D=\tfrac{1}{4}(J_{zz}-J), \quad E=\tfrac{1}{4}(J_{xx}-J_{yy}), \tag{4a}$$

$$\alpha=(J_{zx}+J_{xz})/4\sqrt{2}, \quad \beta=(J_{zx}-J_{xz})/4\sqrt{2}. \tag{4b}$$

For isotropic exchange, $D=E=\alpha=\beta=0$, and we have a ground singlet at $-\frac{3}{4}J$, and an excited triplet at $\frac{1}{4}J$ [see Fig. 4(a)].

For completeness, the relations between our eigenstates and the states of each pseudospin are

$$|1,1\rangle=|+,+\rangle, \quad |1,0\rangle=\tfrac{1}{2}\sqrt{2}[1+,-\rangle+|-,+\rangle], \tag{5}$$
$$|1,-1\rangle=|-,-\rangle, \quad |0,0\rangle=\tfrac{1}{2}\sqrt{2}|[+,-\rangle-|-,+\rangle],$$

where $|+,-\rangle$ represents $|S_1,m_1=\frac{1}{2}\rangle$, $|S_2,m_2=-\frac{1}{2}\rangle$, etc.

2. Zeeman Interaction

In order to examine the Zeeman effect, we first assume that the local symmetry of each Co^{2+} ion is not affected by its neighbor. This is probably a fair assumption for Co^{2+} in ZnF_2, where cobalt and zinc ions have comparable radii, but for MgF_2 it is in doubt. The assumption can be tested in part by a comparison of the g values found from the pair spectrum at high fields with the known single-ion values.

TABLE I. Relative probability of the various possible triads. The designation is indicated in Fig. 5. At 5% concentration the relative proability of all triads with respect to all nnn pairs is 13.5%.

Triad type	Coupled ions	Probability
I	1-2-8	$4c^3(1-c)^{19}$
II	1-2-6	$8c^3(1-c)^{20}$
III	6-2-8	$8c^3(1-c)^{21}$
IV	1-2-3	$4c^3(1-c)^{22}$
V	3-2-8	$4c^3(1-c)^{22}$

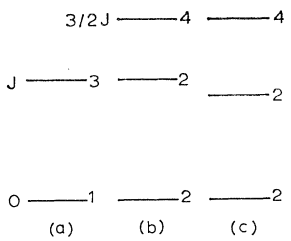

FIG. 4. Energy-level scheme for isotropic exchange interactions: (a) pairs, (b) all types of triads except type I, and (c) type-I triads.

[17] M. E. Lines, Phys. Rev. **137**, A982 (1965).

Under this assumption we have

$$\mathcal{H}_Z=-(\mathbf{M}_1+\mathbf{M}_2)\cdot\mathbf{H}=\mu_B\mathbf{H}\cdot(\mathbf{g}_1\cdot\mathbf{S}_1+\mathbf{g}_2\cdot\mathbf{S}_2), \quad (6)$$

where $\mathbf{M}_1$ and $\mathbf{M}_2$ are the magnetic moments of the ions and H is the magnetic field. For the sites 1 and 2 we have the following relations between the components of the g tensor:

$$\begin{aligned} &g_1^{xx}=g_1^{y'y'}=g_2^{yy}=g^1,\\ &g_1^{yy}=g_1^{x'x'}=g_2^{xx}=g^2,\\ &g_1^{zz}=g_1^{z'z'}=g_2^{zz}=g^3. \end{aligned} \quad (7)$$

The matrix representation of $\mathcal{H}_Z$ in the basis $|S,M_s\rangle$ is

$$\mathcal{H}_Z=\mu_B\begin{pmatrix} g^3H_z & [(g^1+g^2)/2\sqrt{2}]H_- & 0 & [(g^2-g^1)/2\sqrt{2}]H_- \\ [(g^1+g^2)/2\sqrt{2}]H_+ & 0 & [(g^1+g^2)/2\sqrt{2}]H_- & 0 \\ 0 & [(g^1+g^2)/2\sqrt{2}]H_+ & -g^3H_z & [(g^1-g^2)/2\sqrt{2}]H_- \\ [(g^2-g^1)/2\sqrt{2}]H_- & 0 & [(g^1-g^2)/2\sqrt{2}]H_+ & 0 \end{pmatrix}, \quad (8)$$

where $H_\pm=H_x\pm iH_y$.

The eigenvalues of the pair system can now be obtained by a diagonalization of $\mathcal{H}_{ex}+\mathcal{H}_Z$.

We should now make a comment concerning the form of the Zeeman effect when the rigorous symmetry of the pair is taken into account; that is, the symmetry of each ion of the pair is only C_s. It is possible to show for this symmetry that the axis perpendicular to the reflection plane is a principal axis of the g tensor (see Appendix A), but we only know that the two other axes lie in the plane, and they are not necessarily orthogonal. Further, the two Co^{2+} ions no longer have the same crystal field environment, and so the crystal fields will be different, as will the g factors. $\mathcal{H}_Z$ is still given by Eq. (6), but now

$$\begin{aligned} &M_{1y}=g_1^{yy}S_{1y}, \quad M_{2y}=g_2^{yy}S_{2y},\\ &M_{1x}=g_1^{xx}S_{1x}+g_1^{xz}S_{1z}, \quad M_{2x}=g_2^{xx}S_{2x}+g_2^{xz}S_{2z},\\ &M_{1z}=g_1^{zx}S_{1x}+g_1^{zz}S_{1z}, \quad M_{2z}=g_2^{zx}S_{2x}+g_2^{zz}S_{2z}, \end{aligned} \quad (9)$$

where x, y, and z refer to the axes defined for site 2.

There are clearly too many independent parameters to handle in view of the limited amount of spectroscopic information available, and in our interpretation of the results we assume that the local symmetry is still closely D_{2h} and use expression (7). Since we can obtain consistent exchange parameters under various Zeeman conditions using the above assumption, we deduce that it is not too serious a limit in the interpretation.

C. Three Exchange-Coupled Ions

It is possible in this experiment to observe the spectrum of triads of exchange-coupled Co^{2+} ions on neighboring sites. There are many possible types of triads in the unit cell and we briefly indicate in Table I relative probabilities of these (see Fig. 5) in the same way as for pairs. For $c=5\%$, triads of types II and III are most probable; triads of types I, IV, and V are approximately one-half as likely.

The simplest triads are types IV and V, because the symmetry plane of both sets of nnn pairs involved is the same and also the end ions are not significantly coupled directly. Types II and III are complicated by the different symmetry planes for the nnn pairs involved, and type I has a possibly non-negligible exchange coupling (nn) between the end ions.

To discuss the Zeeman Hamiltonian we notice that each triad involves two ions at corner sites and one at the body center (or vice versa), so that we have the same Zeeman Hamiltonian for the above five types of triads, provided, of course, that the site symmetry D_{2h} is not too distorted. Discussing only the simplest triads IV and V, we find exchange and Zeeman Hamiltonians

$$\mathcal{H}_{ex}=(\mathbf{S}_1+\mathbf{S}_3)\cdot\mathbf{J}\cdot\mathbf{S}_2, \quad (10)$$

$$\mathcal{H}_Z=\mu_B\mathbf{H}\cdot[\mathbf{g}_1\cdot\mathbf{S}_1+\mathbf{g}_2\cdot\mathbf{S}_2+\mathbf{g}_3\cdot\mathbf{S}_3], \quad (11)$$

written for triad 1-2-3. J has the same nonzero elements as for the nnn pair, and the elements of the g tensors are

$$\begin{aligned} &g_1^{xx}=g_2^{yy}=g_3^{xx}=g^1,\\ &g_1^{yy}=g_2^{xx}=g_3^{yy}=g^2,\\ &g_1^{zz}=g_2^{zz}=g_3^{zz}=g^3, \end{aligned} \quad (12)$$

with axes x, y, and z defined as for site 2. The matrices representing $\mathcal{H}_{ex}$ and $\mathcal{H}_Z$ are given in Appendix B in the basis $|S_{13},S,M_s\rangle$, where $\mathbf{S}_{13}=\mathbf{S}_1+\mathbf{S}_3$ and $\mathbf{S}=\mathbf{S}_1+\mathbf{S}_2+\mathbf{S}_3$.

Finally, the approximate level scheme may be obtained by assuming that all exchange interactions are isotropic. For all types of triads except I, we have two doublets and a quartet, with energies $-J$, 0, and $\frac{1}{2}J$, respectively [see Figs. 4(b) and 4(c)]. For type I we must introduce a coupling $J_{nn}\mathbf{S}_1\cdot\mathbf{S}_3$, giving two doublets and a quartet again with energies $-J+\frac{1}{4}J_{nn}$, $-\frac{3}{4}J_{nn}$, and $\frac{1}{2}J+\frac{1}{4}J_{nn}$. We now proceed to a discussion of the experimental results.

IV. RESULTS AND INTERPRETATION

The analysis of the results will be carried out in somewhat greater detail for the pairs than for the triads,

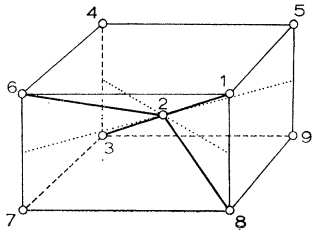

FIG. 5. Triad identification.

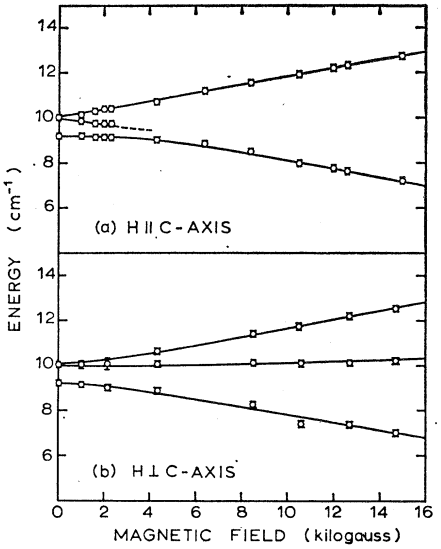

FIG. 6. Pair spectra as a function of magnetic field H: (a) $\mathbf{H}\|(c$ axis) and (b) $\mathbf{H}\perp(c$ axis). The points are experimental results. Solid lines indicate the computed theoretical spectrum. The exchange and Zeeman parameter used are those given in the text.

since the experimental and theoretical position is much clearer. There is no ambiguity as to which type of pair is under examination and the observed spectral lines are approximately twice as intense. Also, we have been unable to resolve the exact behavior of the triad spectra at intermediate magnetic field values because of the experimental resolution limitations and the signal-to-noise ratio problems inherent in this type of spectroscopy.

A. nnn Pairs

In Fig. 6 we show the energy of the observed spectral lines as a function of magnetic field for two different directions with respect to the crystal axes.

1. $H\|(c$ Axis)

From the point of view of symmetry this is the simplest direction for the magnetic field, since here all eight nnn pairs in the unit cell are equivalent. At zero field, two lines are resolved which split to give three observed lines at low fields. The center of gravity of the system is at 9.8 cm^{-1}, and the zero-field splitting of about 1 cm^{-1} indicates that the anisotropic component of the exchange coupling is of the order of 10% of the isotropic component. Bearing this in mind, from matrix (8) it appears that there are only two states of the excited triplet ($S=1$) which have magnetic dipole matrix elements to the ground state, but from matrix (2) it can be seen that anisotropic exchange elements such as α will mix the states $|S=1, M_s=\pm1\rangle$ with $|S=1, M_s=0\rangle$, giving a transition probability for all three states, provided that the level splitting of the triplet is not too great. By contrast, at high fields the states are quite pure and only transitions to states $|S=1, M_s=\pm1\rangle$ will be found. This behavior is quite closely that observed in the experiment; the spectral line corresponding to the state $|1,0\rangle$ becomes too weak to follow as soon as the Zeeman splitting is comparable with the zero-field splitting. The magnitude of the absorption coefficient, in so far as it can be determined with the experimental geometry employed, is what one would expect for normal magnetic dipole transitions. This comes about because the transition matrix elements [see matrix (8)] are of the magnitude $\mu_B(h_x+ih_y)(g^2-g^1)/2\sqrt{2}$ (where h is the infrared magnetic field) and $|g^2-g^1|\approx4$ for Co^{2+} in MgF_2.[16]

At the higher fields employed we may take the slope of the spectral lines to give g^3. We find $g^3=3.92$, which must be compared with the single-ion value of 4.24. We expect the decrease to be partly due to the exchange mixing within the ^4E manifold[17] (Fig. 3), and partly also to the distortion of the local symmetry by the Co^{2+} neighbors.

2. $H\perp(c$ Axis)

From the symmetry it is clear that there are, in general, two inequivalent types of pairs when the field is in the plane normal to the c axis. However, it turns out that the inequivalence is so small that it is not observed in this experiment, where the spectral resolution is about 0.2 cm^{-1}.

For low fields we again see three lines in the spectrum as for $H\|c$, but the magnetic field (H_x,H_y) is now mixing the states [matrix (8)], and this situation is maintained to higher fields as well, giving a continuous three-line spectrum. Figure 7 indicates the allowed transitions for the case

$$\mathcal{H}_{ex}(\text{isotropic})\gg\mathcal{H}_Z\gg\mathcal{H}_{ex}(\text{anisotropic}).$$

The axis for $\mathbf{H}\perp c$ in Fig. 6 is in fact [110]. In this case we may easily evaluate the magnitude of the inequivalence in the spectra of the two types of pairs (types 1-2 and 6-2 of Fig. 2). We find for large H a splitting of $2E$ for the central level and E for the other two. Since no splitting is observed, we deduce that E is small, $E<0.1$ cm^{-1}, and this fits conveniently with the zero-field observation that two states are nearly degenerate.

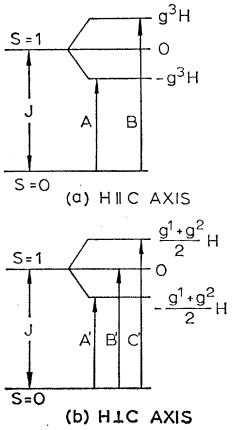

FIG. 7. Zeeman energy-level scheme for pairs: (a) $\mathbf{H}\|(c$ axis) and (b) $\mathbf{H}\perp(c$ axis). The allowed transitions are shown by arrows A, B and A', B', C', respectively.

A point of major interest concerns the value of the antisymmetric component β of the anisotropic exchange tensor. There is no doubt on theoretical grounds that such a term can exist when the symmetry is favorable, but there is only a limited amount of direct experimental evidence for such a term. Such a direct observation would be possible in this experiment, and Co^{2+} is a particularly favorable case. Unfortunately, the antisymmetric component only enters to mix the ground antisymmetric state ($S=0$) with the excited symmetric triplet ($S=1$). Any attempt to evaluate this parameter will depend upon the observation of some upward curvature of the lowest line in the spectrum with $\mathbf{H}\|c$, since this is the simplest and most direct manifestation of such a term. It turns out that we can only follow this line down to about 5 cm^{-1} before its energy becomes suspect due to the low signal-to-noise ratio, and with the given spectral resolution, we would only be able to detect curvature due to a β term of magnitude 0.5 cm^{-1} or greater. No curvature is observed, so we can only conclude that $\beta<0.5$ cm^{-1}. The results of our evaluation of the observed pair spectra are the following:

$$J=9.8(\pm0.1)\ cm^{-1},\quad D=0.2(\pm0.05)\ cm^{-1},$$
$$E=0(\pm0.1)\ cm^{-1},\quad \alpha=0.2(\pm0.05)\ cm^{-1},$$
$$\beta=0(\pm0.5)\ cm^{-1},\quad g^3=3.92,\ \tfrac{1}{2}(g^1+g^2)=3.95.$$

In Fig. 6 we also show the results of a computer diagonalization of the Hamiltonian matrix using the above parameters. With the same values, a computer calculation of the angular dependence in the plane normal to the c axis shows that no inequivalence between the two types of pairs would be observable in our experiment, in agreement with the above conclusions.

We now examine the contributions to the above parameters from magnetic dipole-dipole effects between two Co^{2+} ions. We have

$$\mathcal{H}_{dd}=(\mathbf{M}_1\cdot\mathbf{M}_2)/r^3-3(\mathbf{M}_1\cdot\mathbf{r})(\mathbf{M}_2\cdot\mathbf{r})/r^5, \quad (13)$$

where r is the ionic spacing. Again assuming that the local symmetry of each ion is D_{2h}, we have

$$\mathcal{H}_{dd}=\mu_B{}^2r^{-3}[g^1g^2(1-3x^2/r^2)S_{1x}S_{2x}+g^1g^2S_{1y}S_{2y}+(g^3)^2(1-3z^2/r^2)S_{1z}S_{2z}-(3zx/r^2)g^3(g^1S_{1x}S_{2z}+g^2S_{1z}S_{2x})], \quad (14)$$

where x and z are the components of r in the symmetry plane of the pair. Taking the single-ion g values $g^1=2.3$, $g^2=6.03$, and $g^3=4.24$ and the lattice constants of MgF_2 $a_0=4.66$ Å and $c_0=3.08$ Å, we find the following contribution to the spin-dependent interactions:

$$J_{dd}=0.5\times10^{-2}\ cm^{-1},$$
$$D_{dd}=1.6\times10^{-2}\ cm^{-1},$$
$$\alpha_{dd}=-6\times10^{-2}\ cm^{-1},$$
$$E_{dd}=-7\times10^{-2}\ cm^{-1},$$
$$\beta_{dd}=-3\times10^{-2}\ cm^{-1}.$$

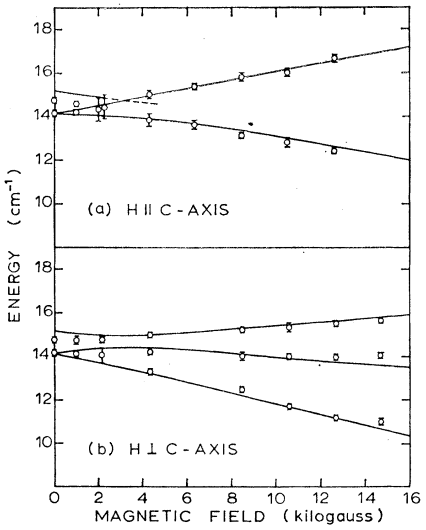

FIG. 8. Triad spectra as a function of magnetic field H: (a) $\mathbf{H}\|(c$ axis) and (b) $\mathbf{H}\perp(c$ axis). The points are experimental results. Solid lines indicate computed results using the parameters obtained from the pair spectrum.

The only case where there is need to modify the interpretation of the exchange values is that of α. We now have a value $\alpha_{ex}=0.26(\pm0.05)$ cm^{-1}. In all other parameters the dipole-dipole contribution is hidden by the experimental error.

B. Triads

In order to discuss the triad spectra we take the view that, as in the case of the nnn pairs, the isotropic component of the exchange energy is dominant. The matrices for $\mathcal{H}_{ex}$ and $\mathcal{H}_Z$ are given in Appendix B, and from them we first note that there will never be transitions from the ground-state doublet to the excited doublet, since the latter is entirely isolated in both matrices. This is fortunate, because any such transition would lie at the same energy as pair transitions and would confuse the picture. On the other hand, transitions are allowed to the quartet and have an energy in the region of $\frac{3}{2}J$ as we observe experimentally, and it is interesting to note that for isotropic exchange, all types of triads (including I) have the same quartet energy.

On the assumption that the anisotropic exchange components can be treated as a perturbation, we now examine the allowed transition to the quartet state.

1. $H\|(c$ Axis)

To zeroth order of perturbation, only two transitions are allowed (Appendix B), and this is essentially the experimental position; also, in this approximation all triads are equivalent. Extra lines may be present in the spectrum at low fields (Fig. 8), as is the case for pairs, but only two lines can definitely be distinguished from the unresolved cluster. A level scheme is given in Fig. 9(a), showing the allowed transitions.

2. $H\perp(c$ Axis)

In this case there are two types of triads with respect to the Zeeman effect. For each type, three transitions are allowed as shown in Fig. 9(b), and in agreement with experiment (Fig. 8). Unfortunately, the experimental restrictions related to the shape of the available crystal have prevented a full analysis of the angular dependence of the triad spectrum.

The triad situation is somewhat complicated and does not lend itself to a simple analysis resulting in further values for the exchange components. The primary reasons for this are the number of inequivalent types when examined in detail, the further distortion of the local symmetry due to three Co^{2+} ions in the MgF_2 host, the weaker experimental spectrum, and the lack of full angular dependence data. Consequently, we merely show, in Fig. 8, that the experimental features of the triad spectrum can be approximately reproduced by a computer diagonalization of the triad Hamiltonian matrices using the exchange parameters and the g parameters obtained from the pair spectrum.

V. COMPARISON WITH EXCHANGE PARAMETERS OF CoF_2

It is of interest to compare the exchange parameters determined in this experiment with those obtained from recent neutron scattering experiments[18] in the ordered antiferromagnet CoF_2, which is isomorphic with MgF_2. We need a theory for a spin-wave spectrum of CoF_2, and we choose first a simple phenomenological model and then examine the more sophisticated theory established by Lines.[17]

A. Simple Model

We take an antiferromagnetic intersublattice exchange Hamiltonian of the form

$$\mathcal{H}_{ex}=J\sum_{j,k}\mathbf{S}_j\cdot\mathbf{S}_k+J'\sum_{j,k}S_{jz}S_{kz}, \tag{15}$$

where both J and $J'>0$, and j and k refer to the opposite sublattices. S_j is a pseudospin $\frac{1}{2}$ associated with the ground Kramers doublet of a Co^{2+} ion on site j, and the summation is over nnn ions only. This model would represent the simplest generalization of our pair Hamiltonian to the whole crystal, taking into account the over-all crystal symmetry and the fact that the spins point along the c axis for CoF_2.[18] The first term in (15) corresponds to the isotropic exchange component, and the second to the anisotropic part.

From (15) we find, in the usual way, a spin-wave dispersion relation

$$E_k=Sz[(J+J')^2-\gamma_k^2J^2]^{1/2}. \tag{16}$$

Here z is the number of nnn, and $\gamma_k=(1/z)\sum_\lambda e^{i\mathbf{k}\cdot\mathbf{R}_\lambda}$, where $\mathbf{R}_\lambda$ defines the vector to a nnn.

[18] R. A. Cowley, P. Martel, and R. W. M. Stevenson, Phys. Rev. Letters **18**, 162 (1967); Can. J. Phys. **46**, 1355 (1968).

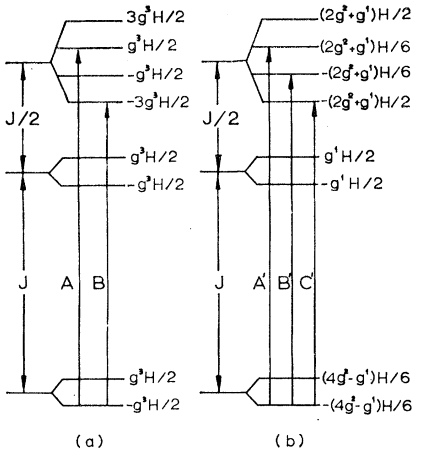

FIG. 9. Zeeman energy-level scheme for triads: (a) $\mathbf{H}\|(c$ axis) and (b) $\mathbf{H}\perp(c$ axis). The allowed transitions are shown by arrows A, B and A', B', C', respectively.

This expression can be used to fit the neutron scattering data, in which case $J=13.3$ cm^{-1} and $J'=2.8$ cm^{-1}, corresponding to a value for our parameter D of 0.7 cm^{-1}.

This simple model neglects the fact that the total exchange interaction, acting on any one ion, is comparable with the excitation energy of the next highest crystal field doublet, which is 152 cm^{-1}.[15] It also neglects nn interactions. Both these effects are taken into account by Lines.[17]

B. Lines's Model of CoF_2

We now have a four-dimensional system, and the crystalline Hamiltonian for each single ion is written

$$\mathcal{H}_{cryst}=\gamma(S_x^2-S_y^2)+\delta S_z^2.$$

The spin $S=\frac{3}{2}$ is the real spin of the Co^{2+} ion if the $^4A_2$ state of D_{4h} symmetry lies lowest, but it is only a pseudospin if the ^4E is in fact lower (see Fig. 3).

According to Lines, the total Hamiltonian for the two sublattices j and k of CoF_2 is

$$\mathcal{H}=\sum_j[\gamma(S_{jy}^2-S_{jx}^2)+\delta S_{jz}^2]+\sum_k[\gamma(S_{kx}^2-S_{ky}^2)+\delta S_{kz}^2]+\sum_{\text{nn}}J_1(\mathbf{S}_j\cdot\mathbf{S}_{j'}+\mathbf{S}_k\cdot\mathbf{S}_{k'})+\sum_{\text{nnn}}J_2\mathbf{S}_j\cdot\mathbf{S}_k. \tag{17}$$

J_1 represents the nn ferromagnetic exchange constant and J_2 the nnn antiferromagnetic constant between spins $\frac{3}{2}$.

Within the context of molecular-field theory, Lines derives the eigenvalues and eigenfunctions of the four levels A, B, C, and D of Fig. 10, so that the presence of C and D is reflected in the states for A and B. He then develops a spin-wave theory limited to A-B excitations and including a fictitious spin $\frac{1}{2}$, thus projecting the spin $S=\frac{3}{2}$ into the subspace A-B $s=\frac{1}{2}$, with the following

relation between S and s:

$$\begin{aligned} S_{jx}&=Ps_{jx}, \quad S_{jy}=Qs_{jy}, \quad S_{jz}=Rs_{jz}+T, \\ S_{kx}&=Qs_{kx}, \quad S_{ky}=Ps_{ky}, \quad S_{kz}=Rs_{kz}-T, \end{aligned} \tag{18}$$

where P, Q, R, and T are dimensionless.

The exchange part of (17) is then

$$\begin{aligned} \mathcal{H}_{ex}=&\sum_{nn} J_1[P^2s_{jx}s_{j'x}+Q^2s_{jy}s_{j'y}+(Rs_{jz}+T)(Rs_{j'z}+T)] \\ &+\sum_{nn} J_1[Q^2s_{kx}s_{k'x}+P^2s_{ky}s_{k'y}+(Rs_{kz}-T)(Rs_{k'z}-T)] \\ &+\sum_{nnn} J_2[PQ(s_{jx}s_{kx}+s_{jy}s_{ky})+(Rs_{jz}+T)(Rs_{kz}-T)]. \end{aligned} \tag{19}$$

From susceptibility and other experimental data Lines deduces

$$\begin{aligned} P=0.99, \quad Q=2.38, \quad R=1.42, \quad T=0.38, \\ J_1=-0.5\ \text{cm}^{-1}, \quad J_2=4.25\ \text{cm}^{-1}. \end{aligned} \tag{20}$$

Our interest lies in the nnn exchange interaction which can be derived from (19) and (20). The isotropic part is $J=J_2PQ=10.0$ cm^{-1}. We might remark here that Lines assumes isotropic exchange between $S=\frac{3}{2}$ spins, which is presumably a good approximation if the orbital singlet $^4A_2$ is low-lying, but not if the ^4E state is lowest, since there would be no reason to assume isotropic exchange between pseudospins $\frac{3}{2}$. Lines's calculation can be used to provide a spin-wave dispersion relation to interpret the neutron scattering data:

$$E_k^2=s^2[a(\zeta_z)b(\zeta_z)-c^2(\zeta)], \tag{21}$$

where

$$\begin{aligned} a(\zeta_z)&=R\rho(R+T/s)+2J_1P^2\cos(2\pi\zeta_z), \\ b(\zeta_z)&=R\rho(R+T/s)+2J_1Q^2\cos(2\pi\zeta_z), \\ c(\zeta)&=8J_2PQ\cos\pi\zeta_x\cos\pi\zeta_y\cos\pi\zeta_z, \end{aligned} \tag{22}$$

and $s=\frac{1}{2}$; $\zeta_{x,y,z}$ are vectors in k space ($\zeta_x=a_0k_x/2\pi$), and

$$\rho=z_2J_2-z_1J_1=8J_2-2J_1.$$

Independently adjusting J_1 and J_2, and retaining the values of P, Q, R, and T, we find an excellent fit to the neutron data,[19] A-B branch ($k\|\langle 001\rangle$), by taking

$$J_1=-1.25\ \text{cm}^{-1}, \quad J_2=4.6\ \text{cm}^{-1}.$$

According to Lines, such values should be decreased by about 5%, giving an isotropic exchange constant (nnn) between spins $\frac{1}{2}$ in CoF_2. $J=PQJ_2=10.3$ cm^{-1}, in good agreement with our spectroscopic value.

It is not easy to say what the errors are in this number, since it has been obtained under various approximations, such as the use of the molecular-field theory to find the wave function for the A-B levels and the use of isotropic exchange interactions between spin $\frac{3}{2}$. However, we might reasonably make the following comparison:

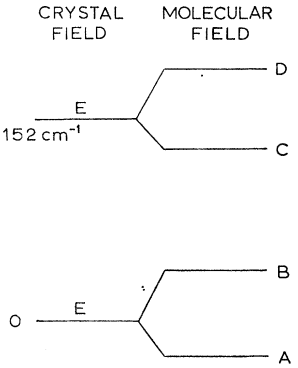

FIG. 10. Energy-level scheme for CoF_2 using molecular-field approximation.

Co^{2+} nnn pairs in MgF_2: $J=9.8$ cm^{-1};
CoF_2 nnn interactions: simple model, $J=13.3$ cm^{-1},
Lines's model, $J=10.3$ cm^{-1}.

VI. CONCLUSIONS

We have presented an account of the far-infrared absorption found in a 5% Co^{2+}-doped crystal of MgF_2. These absorptions are consistent with what is expected for pairs and triads of nnn magnetic ions interacting through an exchange constant of about 10 cm^{-1}. The evidence for such an assignment is found from agreement with calculated transition probabilities, selection rules, and symmetry arguments, particularly with respect to the Zeeman effect. It is felt that such evidence is conclusive in the case of the pair spectrum, but it is admitted that a full analysis of the triad case has not been attempted and all that has been shown is that the observed spectrum is closely the spectrum calculated for triads using the pair exchange and g parameters.

Close numerical agreement has been found for the isotropic exchange value in the case of dilute pairs and the value from CoF_2. However, it is not particularly meaningful to make a detailed comparison extending to the anisotropy of exchange, since the environment of the pair is bound to be somewhat distorted with respect to the concentrated cobalt crystal. This fact has caused considerable difficulty within the experiment iteslf due to the very large numbers of extra parameters introduced. In spite of the foregoing remarks, it should be said that it is a little surprising that Co^{2+} pairs in such a low symmetry should show only 10% anisotropy of exchange. A full evaluation of this question would depend upon an extension of a microscopic theory of exchange interactions such as that of Elliott and Thorpe[8] or of Levy.[7]

The question of antisymmetric anisotropic exchange has not been answered in this paper, because it does not have a particularly direct spectral manifestation. It might prove a worthwhile investigation to attempt to follow the lowest-lying pair Zeeman level into the microwave frequency region where its nonlinearity in field dependence would immediately be a measure of this constant. Of course, it must be recognized that the EPR spectrum of Co^{2+} in MgF_2 does not lend itself to analy-

[19] R. A. Cowley (private communication). Recent corrected values of the neutron data, using Lines's theory, give $J_1=-0.83$ cm^{-1} and $J_2=4.54$ cm^{-1}. The value for J_2 is in good agreement with our result.

sis easily, because of the hyperfine and superhyperfine structure, none of which is resolved in the far-infrared experiment.

An underlying difficulty for the comparison of J values for Co^{2+} is emphasized by Lines's calculation for CoF_2. The first excited Kramers doublet is only separated from the ground state by about 150 cm^{-1}. This means that the Co^{2+} single-ion ground-state wave functions in CoF_2 are different from the dilute case because of exchange mixing with the excited state (the mixing being much greater when eight neighbors are involved rather than two). This not only changes the prediction which one might make for anisotropy constants, supporting our above argument for avoiding such a prediction, but also changes the g values as found in the Zeeman effect.

ACKNOWLEDGMENTS

We wish to acknowledge many conversations with Dr. R. J. Elliott which were most helpful and stimulating. We also acknowledge helpful conversations with Dr. Y. Ayant. The crystals used in this experiment were grown by Dr. D. A. Hukin and B. Davis of the Clarendon Laboratory. The necessary x-ray data were obtained by Mrs. C. Peagram.

APPENDIX A: g-TENSOR PRINCIPAL DIRECTIONS FOR SYMMETRY C_s

The C_s double group has the character table

	E	$\bar{E}$	σ_v	$\bar{\sigma}_v$
Γ_1	1	1	1	1
Γ_2	1	1	−1	−1
Γ_3	1	−1	$-i$	i
Γ_4	1	−1	i	$-i$

The energy levels of a Kramers ion are split into a number of doublets by a crystal field of C_s symmetry, and each doublet is associated with representations Γ_3 and Γ_4.

We take O_z normal to the symmetry plane, and O_x and O_y lying in the plane. We choose two states $|a\rangle$ and $|\bar{a}\rangle$ to make up the ground Kramers doublet such that

$$\sigma_v|a\rangle=-i|a\rangle,$$
$$\sigma_v|\bar{a}\rangle=i|\bar{a}\rangle.$$

Now M is a pseudovector and M_z is invariant with respect to σ_v, so that

$$\langle a|M_z|\bar{a}\rangle=\langle a|\sigma_v^{-1}M_z\sigma_v|\bar{a}\rangle$$
$$=\langle a|\sigma_v^{*}M_z\sigma_v|\bar{a}\rangle=-\langle a|M_z|\bar{a}\rangle=0.$$

Also, we know that M_z is an odd operator with respect to time and has opposite mean values in the two Kramers conjugate states $|a\rangle$ and $|\bar{a}\rangle$:

$$\langle a|M_z|a\rangle=-\langle\bar{a}|M_z|\bar{a}\rangle=\tfrac{1}{2}g^{zz},$$

and therefore

$$M_z=\tfrac{1}{2}g_{zz}\begin{vmatrix}1 & 0\\ 0 & 1\end{vmatrix}=g^{zz}S_z,$$

and O_z is a principal direction of the g tensor. The two other directions lie in the xy plane.

If we now consider the pair 1-2 in Fig. 2, where the y axis is normal to the symmetry plane zox which contains the axis O_z, we now only have to change the basis states for the ground doublet by a similarity transformation to find $M_y=g^{yy}S_y$.

APPENDIX B

The matrix of $\mathcal{H}_{ex}=(\mathbf{S}_1+\mathbf{S}_3)\cdot\mathbf{J}\cdot\mathbf{S}_2$ in the basis $|(S_{13}),S,M_s\rangle$ is

$\left\vert\frac{3}{2},\frac{3}{2}\right\rangle$	$\left\vert\frac{3}{2},\frac{1}{2}\right\rangle$	$\left\vert\frac{3}{2},-\frac{1}{2}\right\rangle$	$\left\vert\frac{3}{2},-\frac{3}{2}\right\rangle$	$\left\vert(0),\frac{1}{2},\frac{1}{2}\right\rangle$	$\left\vert(0),\frac{1}{2}-\frac{1}{2}\right\rangle$	$\left\vert(1),\frac{1}{2},\frac{1}{2}\right\rangle$	$\left\vert(1),\frac{1}{2},-\frac{1}{2}\right\rangle$
$\frac{1}{2}J+2D$	$(2\sqrt{\frac{2}{3}})\alpha$	$(2/\sqrt{3})E$	0	0	0	$(\alpha+3\beta)/\sqrt{3}$	$-(\sqrt{\frac{2}{3}})E$
$(2\sqrt{\frac{2}{3}})\alpha$	$\frac{1}{2}J-2D$	0	$(2/\sqrt{3})E$	0	0	$-\sqrt{2}D$	$\alpha-\beta$
$(2/\sqrt{3})E$	0	$\frac{1}{2}J-2D$	$-(2\sqrt{\frac{2}{3}})\alpha$	0	0	$\beta-\alpha$	$-\sqrt{2}D$
0	$(2/\sqrt{3})E$	$-(2\sqrt{\frac{2}{3}})\alpha$	$\frac{1}{2}J+2D$	0	0	$-(\sqrt{\frac{2}{3}})E$	$-(\alpha+3\beta)/\sqrt{3}$
0	0	0	0	0	0	0	0
0	0	0	0	0	0	0	0
$(\alpha+3\beta)/\sqrt{3}$	$-\sqrt{2}D$	$\beta-\alpha$	$-(\sqrt{\frac{2}{3}})E$	0	0	$-J$	0
$-(\sqrt{\frac{2}{3}})E$	$\alpha-\beta$	$-\sqrt{2}D$	$-(\alpha+3\beta)/\sqrt{3}$	0	0	0	$-J$

where J, α, β, D, and E are defined by Eqs. (3), (4a), and (4b). The relations between these states and those of each psuedospin are

$$\left|\tfrac{3}{2},\tfrac{3}{2}\right\rangle=|+++\rangle,$$
$$\left|\tfrac{3}{2},\tfrac{1}{2}\right\rangle=(1/\sqrt{3})(|-++\rangle+|+-+\rangle+|++-\rangle),$$
$$\left|\tfrac{3}{2},-\tfrac{1}{2}\right\rangle=(1/\sqrt{3})(|+--\rangle+|-+-\rangle+|--+\rangle),$$
$$\left|\tfrac{3}{2},-\tfrac{3}{2}\right\rangle=|---\rangle,$$
$$\left|(0),\tfrac{1}{2},\tfrac{1}{2}\right\rangle=(1/\sqrt{2})(|++-\rangle-|-++\rangle),$$
$$\left|(0),\tfrac{1}{2},-\tfrac{1}{2}\right\rangle=(1/\sqrt{2})(|--+\rangle-|+--\rangle),$$
$$\left|(1),\tfrac{1}{2},\tfrac{1}{2}\right\rangle=(1/\sqrt{6})(-|++-\rangle-|-++\rangle+2|+-+\rangle),$$
$$\left|(1),\tfrac{1}{2},-\tfrac{1}{2}\right\rangle=(1/\sqrt{6})(-|--+\rangle-|+--\rangle+2|-+-\rangle).$$

The matrix of $\mathcal{H}_Z = \mu_B \mathbf{H} \cdot [\mathbf{g}_1 \cdot \mathbf{S}_1 + \mathbf{g}_2 \cdot \mathbf{S}_2 + \mathbf{g}_3 \cdot \mathbf{S}_3]$ in the basis $|(S_{13}), S, M_S\rangle$ is

$$
\left.\begin{array}{cccccccc}
\left|\frac{3}{2},\frac{3}{2}\right\rangle & \left|\frac{3}{2},\frac{1}{2}\right\rangle & \left|\frac{3}{2},-\frac{1}{2}\right\rangle & \left|\frac{3}{2},-\frac{3}{2}\right\rangle & \left|(0),\frac{1}{2},\frac{1}{2}\right\rangle & \left|(0),\frac{1}{2},-\frac{1}{2}\right\rangle & \left|(1),\frac{1}{2},\frac{1}{2}\right\rangle & \left|(1),\frac{1}{2},-\frac{1}{2}\right\rangle \\
3g^3H_z & (\sqrt{\tfrac{1}{3}})(2g^1+g^2)H_x & 0 & 0 & 0 & 0 & (2\sqrt{\tfrac{1}{6}})(g^2-g^1)H_+ & 0 \\
 & -(i\sqrt{\tfrac{1}{3}})(2g^2+g^1)H_y & & & & & & \\
(\sqrt{\tfrac{1}{3}})(2g^1+g^2)H_x & g^3H_z & \frac{1}{3}(4g^1+2g^2)H_x & 0 & 0 & 0 & 0 & \frac{1}{3}\sqrt{2}(g^1-g^2)H_+ \\
+(i\sqrt{\tfrac{1}{3}})(2g^2+g^1)H_y & & -i\frac{1}{3}(4g^2+2g^1)H_y & & & & & \\
0 & \frac{1}{3}(4g^1+2g^2)H_x & -g^3H_z & (\sqrt{\tfrac{1}{3}})(2g^1+g^2)H_x & 0 & 0 & \frac{1}{3}\sqrt{2}(g^1-g^2)H_- & 0 \\
 & +i\frac{1}{3}(4g^2+2g^1)H_y & & -(i\sqrt{\tfrac{1}{3}})(2g^2+g^1)H_y & & & & \\
0 & 0 & (\sqrt{\tfrac{1}{3}})(2g^1+g^2)H_x & -3g^3H_z & 0 & 0 & 0 & (2/\sqrt{6})(g^2-g^1)H_- \\
 & & +(i\sqrt{\tfrac{1}{3}})(2g^2+g^1)H_y & & & & & \\
0 & 0 & 0 & g^3H_z & -g^2H_x+ig^1H_y & 0 & 0 & 0 \\
0 & 0 & 0 & -g^2H_x-ig^1H_y & -g^3H_z & 0 & 0 & 0 \\
(2\sqrt{\tfrac{1}{6}})(g^2-g^1)H_- & 0 & \frac{1}{3}\sqrt{2}(g^1-g^2)H_+ & 0 & 0 & 0 & \frac{1}{3}(-4g^1+g^2)H_x & \frac{1}{3}(-4g^1+g^2)H_x \\
 & & & & & & -i\frac{1}{3}(4g^2-g^1)H_y & +i\frac{1}{3}(4g^2-g^1)H_y \\
0 & \frac{1}{3}\sqrt{2}(g^1-g^2)H_- & 0 & (2/\sqrt{6})(g^2-g^1)H_+ & 0 & 0 & -g^3H_z & -g^3H_z
\end{array}\right\} \times \tfrac{1}{2}\mu_B.
$$